PUBLICATION IV

Momentum transport studies in JET H-mode discharges with an enhanced toroidal field ripple

In: Plasma Physics and Controlled Fusion 52, 065004 (11 pp), 2010.

http://iopscience.iop.org/0741-3335/52/6/065004/pdf/0741-3335_52_6_065004.pdf

Plasma Phys. Control. Fusion **52** (2010) 065004 (11pp) doi:10.1088/0741-3335/52/6/065004

Momentum transport studies in JET H-mode discharges with an enhanced toroidal field ripple

P C de Vries[1,2], T W Versloot[2], A Salmi[3], M-D Hua[4], D H Howell[1], C Giroud[1], V Parail[1], G Saibene[5], T Tala[6] and JET EFDA Contributors[7]

JET-EFDA Culham Science Centre, Abingdon, OX14 3DB, UK
[1] EURATOM/CCFE Association, Culham Science Centre, Abingdon, OX14 3DB, UK
[2] FOM institute for Plasma Physics Rijnhuizen, Association EURATOM-FOM, PO Box 1207, Nieuwegein, The Netherlands
[3] Association Euratom-Tekes, Helsinki University of Technology, PO Box 4100, 02015 TKK, Finland
[4] Imperial College, SW7 2BY, London, UK
[5] Fusion for Energy Joint Undertaking, 0819 Barcelona, Spain
[6] Association Euratom-Tekes, VTT, PO Box 1000, 02044 VTT, Finland

E-mail: Peter.de.Vries@jet.efda.org

Received 20 November 2009, in final form 29 March 2010
Published 27 April 2010
Online at stacks.iop.org/PPCF/52/065004

Abstract
In this study, enhancement of the toroidal field (TF) ripple has been used as a tool in order to reveal the impact of the momentum pinch on the rotation profiles in H-mode JET discharges. The analysis showed that flatter rotation profiles were obtained in discharges with a high TF ripple, attributed to a smaller inward momentum convection. An average inward momentum pinch of approximately $V_p \approx 3.4\,\mathrm{m\,s^{-1}}$ and a normalized pinch value of $RV_p/\chi \approx 6.6$ could explain the observation. The data show that the momentum at the edge affects the peaking of the rotation and momentum density profiles. Under the assumption that the heat and momentum diffusivities are equal, an estimate of the levels of the momentum pinch in all discharges in the JET rotation database was made. For H-mode discharge these ranged from $0.3\,\mathrm{m\,s^{-1}} < V_p < 17\,\mathrm{m\,s^{-1}}$, with $2 < RV_p/\chi < 10$. A larger momentum pinch was found in discharges with a smaller density profile gradient length, i.e. a more peaked density profile.

(Some figures in this article are in colour only in the electronic version)

1. Introduction

The study of plasma rotation and momentum transport has gained interest over the last few years as rotation is thought to play an important role in the stability of tokamak plasmas. Furthermore,

[7] Annex to Romanelli F 2008 *Proc. 22nd IAEA Conf. on Fusion Energy 2008 (Geneva, Switzerland, 2008)* (Vienna: IAEA).

0741-3335/10/065004+11$30.00

it may affect transport properties via the stabilization of turbulence. A proper understanding of all aspects that affect the rotation of tokamak plasmas, in particular momentum transport and rotation sources, is therefore important if one wants to make an accurate prediction of the rotation in ITER.

Momentum transport was previously assumed to be closely linked to the transport of energy and hence in modelling predictions rotation profiles were thought to be similar to those of the temperature [1, 2]. It was shown, however, that such an assumption does not hold and effective energy and momentum diffusivities can differ significantly. The effective Prandtl number, i.e. the ratio of effective momentum and energy diffusivities, was found to be below unity in the core of JET plasmas [3, 4]. Furthermore, the global energy and momentum confinement times were not always equal and their ratio was found to increase with decreasing average rotation. Many of these aspects may be linked to the presence of a momentum pinch [5, 6]. Past experiments already indicated a convective component in momentum transport [7–9], while evidence for a momentum pinch has been found from experiments in various devices [10–13]. Beside these transport issues one needs to understand the sources of rotation. Generally considerable toroidal rotation has been observed in plasmas with tangential neutral beam injection (NBI), for which the momentum transfer from the injected particles to the bulk plasma seems to be reasonably well understood [14]. This picture is, however, complicated in the presence of a large toroidal field (TF) ripple which via non-ambipolar losses of fast (NBI) ions strongly influences the torque on the plasma [15]. Plasma rotation has also been observed in plasmas with no external momentum sources [16, 17] or those with balanced NBI [18], suggesting the presence of possible intrinsic momentum sources.

This paper will not deal in detail with mechanisms of TF ripple induced torque on the plasma but utilize TF ripple as a tool, in order to reveal the impact of the momentum pinch on the rotation profiles in H-mode JET discharges. The observations will be placed in the context of earlier studies done at JET [3, 4, 11]. The details of these specific experiments will be described in section 2. Thereafter, in section 3, the momentum transport properties of these discharges will be studied and compared with that of the energy. In section 4 it will be shown that an inward momentum pinch can explain the observations. The momentum pinch for these H-mode discharges will be determined and the magnitude of this pinch is estimated for all entries in the JET rotation database [4]. The last section will summarize the conclusions.

2. Description of the experiments

Standard operations at JET are carried out with a set of 32 TF coils all carrying equal current. But at JET it is possible to vary the TF ripple amplitude by independently powering the 16 odd and 16 even-numbered coils. The imbalance current between the two coil sets can be changed in a controlled way increasing the TF ripple. The TF ripple amplitude, δ_{B_T}, is defined as the relative amplitude of the magnetic field variation: $\delta_{B_T} = (B_{max} - B_{min})/(B_{max} + B_{min})$. The values quoted in this paper give the maximum amplitude in the plasma, found near the mid-plane ($z = 0$) at the low-field-side separatrix.

A series of experiments were performed to investigate the impact of the TF ripple on the H-mode pedestal properties [19, 20] for which the TF ripple was increased from the standard JET level of $\delta_{B_T} = 0.08\%$ up to 1.0%. This paper will discuss the characteristics of the rotation profiles and momentum transport in these experiments. In total, 16 discharges were analysed which were standard type I ELMy H-modes with a plasma current of $I_p = 2.6$ MA, a toroidal magnetic field of $B_T = 2.2$ T and $q_{95} = 3$, using a plasma configuration with a low triangularity and standard elongation ($\delta = 0.23, k = 1.65$). The auxiliary heating came from NBI only, which in JET is injected near tangentially, in the direction of the plasma current.

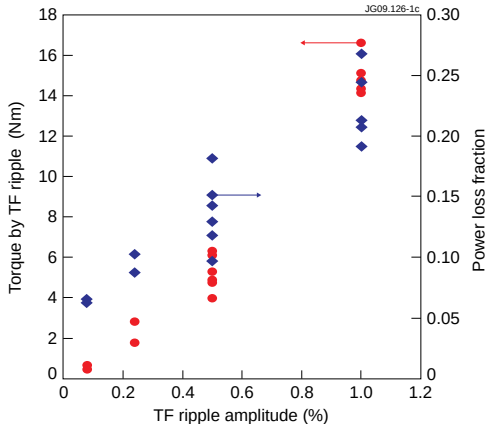

Figure 1. The power loss fraction (diamonds) and TF ripple induced counter-current torque (circles) as calculated by ASCOT for the series of discharges to be studied in this paper.

The NBI power ranged from 13 to 19 MW and supplied a toroidal torque of the order of 15 N m. Generally, these plasmas had equal ion and electron temperatures ($T_i/T_e \sim 1$) and density profiles with a typical inverse gradient length of $R/L_n \sim 2$. These H-mode plasmas can furthermore be characterized by the main global dimensionless parameters; normalized collisionality ($\nu^* = 0.007$–0.01), normalized Larmor radius $\rho^* = 2 \times 10^{-4}(0.02\%)$ and normalized β ($\beta_N = 1.7$–2.0). The effective charge of these plasmas was $Z_{eff} = 1.5 \pm 0.2$.

The TF ripple breaks the axi-symmetry of the magnetic field and enhances particle losses, in particular energetic ions, such as alpha particles created in fusion reactions or those injected by NBI. The non-ambipolar ion losses have a significant effect on the plasma rotation as have been shown experimentally [15, 21]. For the purpose of transport studies it is important to understand the energy and momentum sources, or torque deposition profiles, which will be affected by the varying TF ripple. An orbit-following Monte Carlo code, ASCOT, was used to determine the TF ripple induced losses of NBI ions, the details of which are described in [22]. In this way it was possible to calculate the fraction of NBI power that was lost and how much toroidal torque was induced due to the TF ripple losses. For TF ripple values up to $\delta_{B_T} = 1.0\%$, the dominant contribution to the TF ripple induced torque is due to its effect on fast ions, injected by NBI, and trapped in banana-orbits and not those actually trapped in the TF ripple [15]. ASCOT analysis has shown that the fraction of particles trapped in the TF ripple is negligible. The torque due to the TF ripple is directed in the counter-current direction and hence opposes the co-current NBI torque. In the calculation of the torque deposition used in this paper, only the effect of the TF ripple on fast ions has been considered.

In figure 1, the power loss fraction and the TF ripple induced total torque, as calculated by ASCOT, are plotted as a function of TF ripple amplitude for all discharges used in this study. It can be seen that for $\delta_{B_T} = 1.0\%$ approximately 20–25% of all NBI power is not absorbed in the plasma but deposited on plasma-facing components. The effect on the rotation will be more pronounced, as the TF ripple induced torque for $\delta_{B_T} = 1.0\%$ is of the same magnitude as, but opposing, the torque supplied by the NBI. Hence the net torque on the plasma for this TF ripple amplitude is near zero. This does not mean that the entire plasma experiences a counter-current torque. In figure 2(*a*) the total torque deposition profiles as calculated by ASCOT are

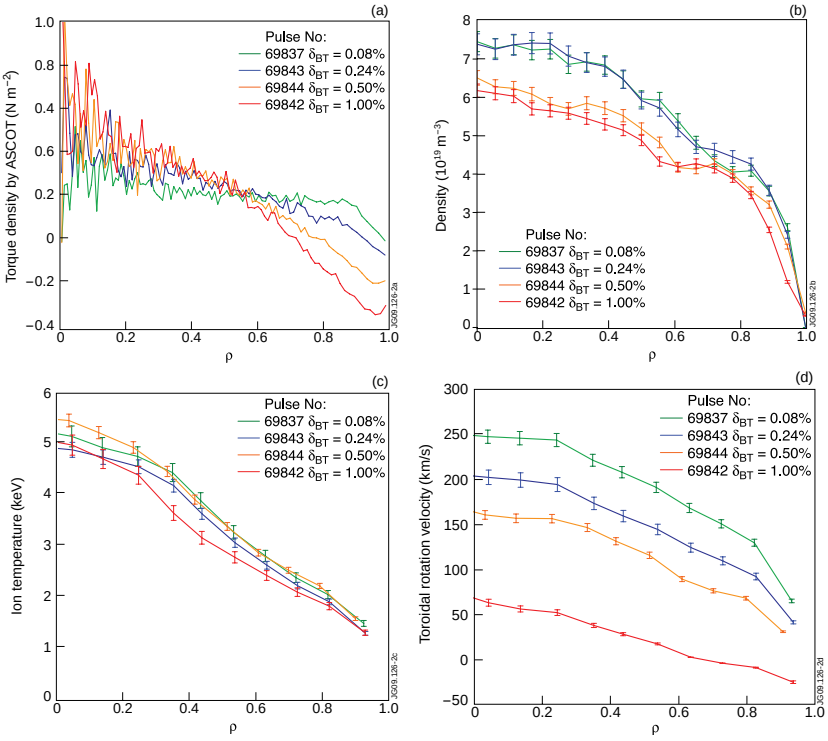

Figure 2. (*a*) The torque deposition profiles as calculated by ASCOT for four similar discharges but with different TF ripple amplitudes. (*b*) The corresponding density profiles measured by the LIDAR Thomson scattering diagnostic. (*c*) The ion temperature profiles measured by CXRS. (*d*) The toroidal rotation profiles measured by the same diagnostic.

shown for four discharges with different TF ripple amplitudes. The increased TF ripple causes a region with counter-current torque near the outer part of the plasma. However, the torque deposited in the core ($\rho < 0.5$) is largely unaffected. Actually, in order to compensate for the TF ripple induced power losses and keep the total absorbed power constant, the requested NBI power was often higher for the higher TF ripple cases, resulting in a higher torque density in the core.

For the same four discharges the electron density, measured by the LIDAR Thomson scattering diagnostic, and ion temperature and toroidal rotation, measured by charge exchange spectroscopy (CXS), are shown in figures 2(*b*)–(*d*). The profiles are plotted versus the normalized radius, ρ. As has been reported earlier, the increase in TF ripple affected the density profiles by lowering the density [20]. The pulses with the highest TF ripple had a lower stored energy ($\beta_N = 1.7$) as well as a lower ν^*. The core ion temperature profiles seem unaffected by the changes in TF ripple, while it has a strong effect on the rotation profiles. Not only does the increase in TF ripple push the plasma rotation at the edge in the counter-current direction, the gradient of the rotation profile is reduced significantly (by approximately a factor 4 from $\delta_{B_T} = 0.08\%$ up to 1.0%). Such a large reduction in rotation gradient and lower

momentum density, while the deposited torque inside $\rho < 0.5$ is actually larger, suggests that the momentum transport differs strongly for these cases.

3. Momentum transport properties

Experiments have shown that TF ripple affects the plasma performance, mainly by a change in the H-mode pedestal [19, 20]. However, its effect on the plasma rotation and momentum transport seems to be significantly larger. This paper will not deal with the detailed effects of TF ripple on the general plasma performance but will compare the momentum transport with the energy transport properties of these discharges.

In order to determine the effective momentum, χ_ϕ^{eff}, and ion heat, $\chi_{\text{i}}^{\text{eff}}$, diffusivities, both the gradients and the sources have to be determined using steady-state power and momentum balance equations, assuming purely diffusive transport:

$$Q_{\text{i}} = -\chi_{\text{i}}^{\text{eff}} n \nabla T_{\text{i}}, \tag{1}$$

$$\Gamma_\phi = -\chi_\phi^{\text{eff}} \nabla \Omega, \tag{2}$$

where Q_{i} is the ion heat flux, Γ_ϕ is the torque flux (i.e. the amount of torque deposited within a certain region divided by the surface), as determined by the ASCOT code, and ∇T_{i}, $\nabla\Omega$ are the gradients in the ion temperature and momentum density, respectively. To begin with, all values are calculated at mid-radius ($\rho = 0.5$) averaged over the gradient region from $\rho = 0.3$–0.7. In order to further reduce the error bars on the gradients, the profiles have been averaged over a large time window of 2 s in which the plasmas were in quasi-steady state. Nevertheless, the error in the diffusivities was still of the order of 30%. It was found that the heat diffusivity varied from $0.92\,\text{m}^2\,\text{s}^{-1} < \chi_{\text{i}}^{\text{eff}} < 1.8\,\text{m}^2\,\text{s}^{-1}$ although for most discharges the value was close to the average of $\chi_{\text{i}}^{\text{eff}} = 1.3\,\text{m}^2\,\text{s}^{-1}$. The variation in core heat diffusivity may be attributed to the changes in density between the pulses. However, a much larger variation was found for the effective momentum diffusivity. The Prandtl number, P_r, can be used to compare the relative changes between both diffusivities. The effective Prandtl number is defined as

$$P_r^{\text{eff}} = \frac{\chi_\phi^{\text{eff}}}{\chi_{\text{i}}^{\text{eff}}}. \tag{3}$$

In figure 3 it can be seen that for low TF ripple amplitudes, again effective Prandtl numbers of about 0.2–0.3 are found, similar to standard JET discharges [3, 4], but this increases to around unity when the TF ripple is increased to $\delta_{B_{\text{T}}} = 1.0\%$.

Although the TF ripple affects the torque on the plasma, its effect for an amplitude of $\delta_{B_{\text{T}}} = 1.0\%$ only reaches up to $\rho > 0.6$ as can be seen from figure 2(*a*). As mentioned above, the torque deposited in the core ($\rho < 0.5$) slightly increases with TF ripple for this dataset. Hence it is not the momentum source that is changing with TF ripple but the effective diffusivity that flattens the rotation profiles as seen in figure 2(*d*). The increase in TF ripple results in a reduction in edge rotation. If the effective Prandtl number is plotted versus the rotation, as shown in figure 3(*b*), the trend suggests that with a larger rotation in the outer part of the plasma, one will have a smaller effective Prandtl number. The effective momentum diffusivity is increased with respect to the heat diffusivity, when a larger TF ripple results in a smaller momentum in the outer part of the plasma.

Besides looking at the local diffusivities, one can compare the global energy and momentum confinement times. Here, the energy confinement time is defined as the total integrated kinetic energy divided by the absorbed power, while the momentum confinement time is the total angular momentum divided by the total torque on the plasma. The ratio of the

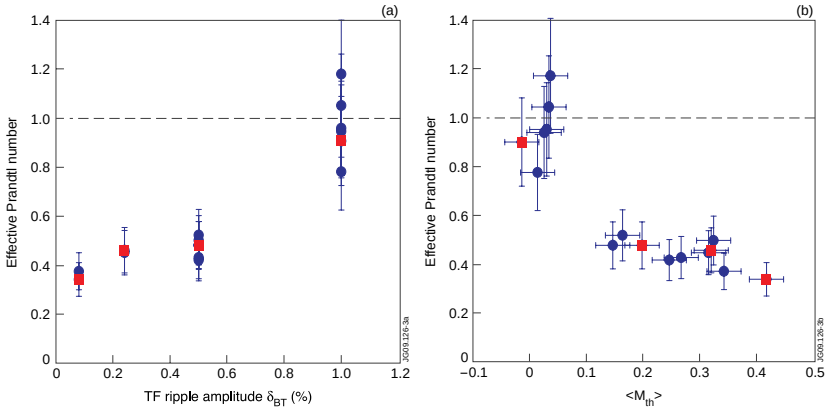

Figure 3. (*a*) The effective Prandtl number versus the TF ripple amplitude. (*b*) The effective Prandtl number versus average thermal Mach number at $\rho = 0.55$. The four discharges from figure 2 are marked by the red squares.

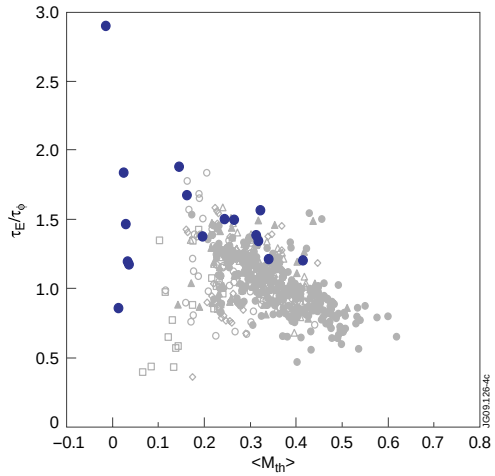

Figure 4. The ratio of the energy and momentum confinement time versus the average thermal Mach number for these TF ripple H-mode discharge (blue dots). The Mach number decreases for increasing TF ripple. In grey the points are from the JET rotation database as in figure 8(*c*) in [4].

two is plotted in figure 4 versus the average thermal Mach number similarly as in figure 8(*c*) of [4]. The thermal Mach number is determined by normalizing the plasma velocity to the thermal velocity [4]. The data follow the main trend found in the JET rotation database: the ratio of energy and momentum time increases with decreasing average Mach number. The energy and momentum confinement time are approximately equal for those discharges with a low TF ripple. However, for the high TF ripple cases, and low to zero edge rotation, the momentum confinement time worsens and is found to be much smaller than the energy confinement.

The momentum confinement time for discharges with TF ripple of $\delta_{B_T} = 1.0\%$ shows a large variation. This causes the break in the trend seen in figure 4, where the ratio for the low Mach number cases seems to be lower. This may be due to an inaccuracy in the calculated torque on these plasmas. For these TF ripple amplitudes, the ripple induced counter-current torque approaches that supplied by the NBI system, resulting in a near zero net torque on the plasma. The data suggest that this net torque, as determined by ASCOT, may be slightly overestimated (roughly by 2–4 N m). Similar issues have been presented when operating with balanced NBI in DIII-D with the suggestion of the presence of an intrinsic torque [18]. The discrepancy shown here could be attributed to differences in the levels of rotation in Ohmic plasmas at larger TF ripple [23] or possibly thermal ion losses [15] or neo-classical toroidal viscosity [24] which is not included in the ASCOT calculations of the torque. Larger TF ripples may also affect thermal particle orbits, enhancing the neo-classical toroidal viscosity [24]. This effect was estimated for two discharges with a TF ripple of $\delta_{B_T} = 1.0\%$, and 0.5%, using the equations in [24] and found to depend strongly on $Z_{\rm eff}$. The torque due to neo-classical viscosity was of the order of about 3 N m for $Z_{\rm eff} \sim 1.5$. But because it is always difficult to accurately determine the effective charge of the plasma, a rather large uncertainty remains.

4. Estimation of the effect of the momentum pinch

Usually the effective Prandtl number in JET H-mode discharges is well below unity. Here the effective momentum diffusivity was found to increase with respect to the ion heat diffusivity when the (edge) rotation was reduced due to the larger TF ripple. The question is, however, whether momentum transport is purely diffusive. The observations can be explained by including an inward convection term to the momentum transport as

$$\Gamma_\phi = -\chi_\phi \nabla\Omega - V_{\rm p}\Omega. \tag{4}$$

Here the symbols Ω and $\nabla\Omega$ represent the momentum density and its gradient, $V_{\rm p}$ is the inward pinch velocity. One may question whether one has to take into account possible intrinsic sources by adding an additional term in equation (4), independent of the velocity or its gradient. This may originate from, for example, residual stress [25] or up–down asymmetries in the equilibrium [26]. The latter may be of less relevance because of the symmetric, low triangularity, plasma configurations used in these experiments. In any case at JET the intrinsic rotation is usually at least one order of magnitude smaller than that in predominantly NBI heated discharges [4, 27]. Hence in equation (4) a possible intrinsic momentum flux, independent of the velocity or its gradient, could be neglected with respect to the flux supplied by NB (Γ_ϕ). The momentum diffusivity, χ_ϕ, contrasts with the effective momentum diffusivity, $\chi_\phi^{\rm eff}$, calculated by equation (2). The presence of an inward convection reduces the effective momentum diffusivity $\chi_\phi^{\rm eff}$ with respect to χ_ϕ [27]. It is clear from equation (4) that a smaller momentum density Ω (in the outer part of the plasma) would reduce the inward convection flux. Hence, in these cases, such as with a large TF ripple ($\delta_{B_T} \sim 1.0\%$), $\chi_\phi^{\rm eff}$ may approach χ_ϕ which may be similar to $\chi_{\rm i}$. While when a significant inward convection is present one obtains an effective Prandtl number smaller than unity. This is indeed what was found in figure 3. Similarly a reduction in the inward convection term (by increasing the TF ripple) will result in a lower momentum confinement time with respect to that of the energy as found in figure 4.

$V_{\rm p}\Omega$ is a parameter that can be indirectly altered by the TF ripple. One can rewrite equation (4) by normalizing it by Γ_ϕ the torque flux, removing the variations in the central deposited torque from discharge to discharge. Because of the small values of Ω in the discharges

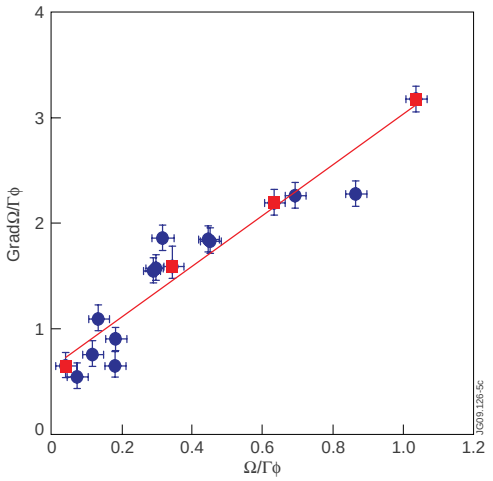

Figure 5. The normalized gradient, $\nabla\Omega/\Gamma_\phi$, for the series of discharges in which the TF ripple was varied between $\delta_{B_T} = 0.08$ and 1%, plotted versus the normalized momentum density, Ω/Γ_ϕ. The red line is a fit through the data points with a slope of 2.19 and an off-set of 0.66. The four discharges from figure 2 are marked by the red squares.

with a high TF ripple, normalization by Ω was found to be impractical. This gives

$$\frac{\nabla\Omega}{\Gamma_\phi} = -\frac{V_p}{\chi_\phi}\frac{\Omega}{\Gamma_\phi} - \frac{1}{\chi_\phi}. \tag{5}$$

In figure 5 the above equation has been plotted for the 16 discharges. As before, these parameters have been determined at $\rho = 0.5$ averaged from $\rho = 0.3$–0.7. The normalized gradient, $\nabla\Omega/\Gamma_\phi$, clearly scales with the normalized momentum density Ω/Γ_ϕ. Note that according to equation (2) the normalized gradient on the y-axis is also equal to χ_ϕ^{eff}. The slope is determined by the magnitude of the pinch velocity, while the off-set is equal to $1/\chi_\phi$. This gives an estimate of the average pinch velocity and momentum diffusivity of this set of discharges. An important parameter is the average normalized pinch velocity, $RV_p/\chi_\phi \sim 6.6$, where R is the major radius, which can be compared with the theoretical predictions [5]. The average pinch velocity was found to be $\langle V_p\rangle = 3.4\pm0.2\,\text{m s}^{-1}$, while the average momentum diffusivity was $\chi_\phi = 1.5 \pm 0.2\,\text{m}^2\,\text{s}^{-1}$. The latter parameter is close to the average ion heat diffusivity of $\chi_i^{\text{eff}} \sim 1.3\,\text{m}^2\,\text{s}^{-1}$ for these discharges. Hence the diffusive transport of momentum was found to be approximately the same as the energy diffusivity as predicted by gyro-kinetic calculations. As was pointed out above, there is some variation from discharge to discharge and it is likely that this is the same for momentum. Nevertheless, the data from figure 5 give an estimate of the average momentum pinch and diffusivity to explain the changes in the rotation profiles with varying TF ripple. It should be pointed out that the near zero values of Ω or $\langle M_{\text{th}}\rangle$ are obtained at $\rho = 0.5$, with the outer part rotating in the counter-current direction while the core rotates in the same direction of the plasma current (and NBI injection).

The above analysis provides a profile averaged momentum pinch over the gradient region of the plasmas. In order to get an idea of the radial profile of the pinch velocity one can redo the analysis for a smaller inner region (i.e. $\rho = 0.10$–0.45) and an outer region (i.e. $\rho = 0.65$–0.90), albeit increasing the error in the determination of the gradients. As shown in figure 6, the slope and thus also the normalized momentum pinch for the outer region are close

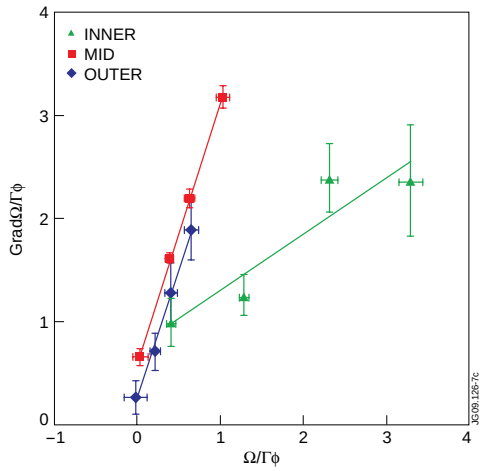

Figure 6. The normalized gradient, $\nabla\Omega/\Gamma_\phi$, for the four discharges in which the TF ripple was varied between $\delta_{B_T} = 0.08$ and 1%, plotted versus the normalized momentum density, Ω/Γ_ϕ. The red squares show the similar analysis as in figure 5, using gradients averaged over the mid-region of the plasma ($\rho = 0.4$–0.8), while the green triangles and blue diamonds are calculated for an inner ($\rho = 0.10$–0.45) and outer ($\rho = 0.65$–0.90) region, respectively.

to the averaged value found for the entire (mid) gradient region, with $RV_p/\chi_\phi \sim 7.5$, while the off-set is lower, indicating a larger diffusivity, of $\chi_\phi = 4 \pm 0.6\,\mathrm{m^2\,s^{-1}}$. The normalized pinch for the inner region is significantly smaller, $RV_p/\chi_\phi \sim 1.6$ with a value for the diffusivity of $\chi_\phi = 1.3 \pm 0.3\,\mathrm{m^2\,s^{-1}}$. Thus, near the outer part of the plasma the momentum pinch velocity is of the order of $V_p = 10\,\mathrm{m\,s^{-1}}$ and this value decreases towards the plasma centre, a profile similar to that found in previous experimental results [11].

A detailed database to study the scaling of rotation and momentum transport in JET discharges has been created [4]. The database contains entries from various operational scenarios, such as type I and III ELMy H-modes or plasmas with internal transport barriers (ITBs) for which the average rotation and momentum source and transport properties are determined in steady-state phases of the discharge. All the entries have a standard TF ripple ($\delta_{B_T} = 0.08\%$) and generally effective Prandtl numbers considerably less than unity. If one considers the observations in the TF ripple experiments and assumes the presence of an inward momentum pinch and that $\chi_\phi \equiv \chi_i^{\mathrm{eff}}$, one can estimate the magnitude of such a pinch by rewriting equations (2), (3) and (4) as

$$\frac{V_p}{\chi_i^{\mathrm{eff}}} \approx (1 - P_r^{\mathrm{eff}})\frac{\nabla\Omega}{\Omega}. \tag{6}$$

Using this equation the normalized momentum pinch, RV_p/χ_ϕ, was calculated for all database entries, averaged over $\rho = 0.3$–0.7, as shown in figure 7. Higher values are found in discharges with more peaked density profiles (i.e. a larger R/L_n). The magnitude and scaling are close to the one predicted by the theory [5]: $RV_p/\chi = 4 + (R/L_n)$. The normalized momentum density gradient ($\nabla\Omega/\Omega$) used in equation (6) was found to be predominantly determined by the gradient in the rotation profile, and the density gradient played only a minor role. Figure 7 gives an idea of the levels of the average momentum pinch in JET plasmas. The values found for the TF ripple experiments match nicely within the other H-mode entries in the database.

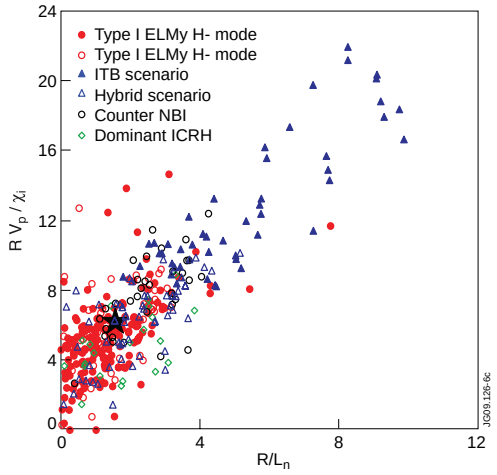

Figure 7. The normalized pinch velocity $RV_{\rm p}/\chi_{\rm i}$ calculated for the entire JET rotation database [4] for various operational scenarios, under the assumption that $\chi_\phi = \chi_{\rm i}$ plotted versus the normalized inverse density gradient length $R/L_{\rm n}$. Note that all parameters in the JET rotation database are determined at $\rho = 0.5$ (averaged from $\rho = 0.2$–0.7). The black star gives the result obtained from the analysis of the TF ripple experiments.

5. Conclusions

Previously the presence of a momentum pinch has been deduced from various experiments [10–13]. It should be said that the power balance analysis presented here does not independently prove the presence of such a pinch. Nevertheless, it was shown that an inward convection component in the momentum transport equation would nicely explain the behaviour of the rotation profiles when the TF ripple was enhanced and the edge rotation was reduced. Moreover, effective Prandtl numbers increased to values close to unity when the inward convection was significantly reduced. This indicates that the small effective Prandtl numbers found in standard JET discharges are caused by the smaller effective momentum transport due to the inward momentum convection. It also explains why in JET the ratio of the energy and momentum confinement scaled with the rotation itself. The experiments clearly showed the significant impact of the momentum pinch on the toroidal rotation profiles in JET H-mode discharges.

The profile average pinch velocity that explained the effects found in these H-mode discharges was $V_{\rm p} = 3.4\,{\rm m\,s^{-1}}$ which is smaller than the maximum found in detailed torque modulation experiments [11]. However, the experimental parameters (e.g. density, heating power and q-profile) differed between these experiments. The density in these H-mode discharges was significantly higher and the heat diffusivity lower than in the modulation experiments. A better comparison would be the normalized pinch velocity, that was found to be $RV_{\rm p}/\chi_\phi \sim 6.6$, which is close to the earlier experiments at JET. Moreover, the magnitude and the observed scaling with the density gradient length match well the theoretical predictions [5].

An estimation of the momentum pinch was made for all entries in the JET rotation database by assuming that $\chi_\phi \approx \chi_{\rm i}$ and the difference between the measured $\chi_\phi^{\rm eff}$ and $\chi_{\rm i}^{\rm eff}$ is due to the momentum pinch. This shows similar values as found from the analysis of the TF

ripple experiments, for H-mode discharges ranging from $0.3\,\mathrm{m\,s^{-1}} < V_\mathrm{p} < 17\,\mathrm{m\,s^{-1}}$, with approximately $2 < RV_\mathrm{p}/\chi < 10$. An increasing trend with the peaking of the density profile was found.

It is interesting to note that for discharges with no or little rotation at the edge the effective diffusivities of heat and momentum were approximately equal in the core, but the momentum confinement time was more than a factor of 2–3 times less than that of the energy. The fact that the transport of energy and momentum in the core is the same, while the global confinement is different, suggests that the edge may have different impacts on the confinement of momentum than on the energy. This could be due to a difference in transport properties, additional drag or losses near the edge of the plasma. These are factors that need to be understood when one would like to accurately predict rotation levels in ITER as the edge rotation may affect the whole profile.

Acknowledgments

This research has been performed under the European Fusion Development Agreement and was partly funded by the Culham Centre for Fusion Energy, the UK Engineering and Physical Sciences Research Council and by the European Communities under contract of association between EURATOM and CCFE. The views and opinions expressed herein do not necessarily reflect those of the European Commission.

References

[1] Scott S D *et al* 1990 *Phys. Rev. Lett.* **64** 531
[2] Mattor N and Diamond P 1988 *Phys. Fluids* **31** 1180
[3] de Vries P C *et al* 2006 *Plasma Phys. Control. Fusion* **48** 1693
[4] de Vries P C *et al* 2008 *Nucl. Fusion* **48** 065006
[5] Peeters A G, Angioni C and Strintzi D 2007 *Phys. Rev. Lett.* **98** 265003
[6] Hahm T S *et al* 2007 *Phys. Plasmas* **14** 072302
[7] Nagashima K *et al* 1994 *Nucl. Fusion* **34** 449
[8] Ida K *et al* 1995 *Phys. Rev. Lett.* **74** 1990
[9] Lee W D *et al* 2003 *Phys. Rev. Lett.* **91** 205003
[10] Yoshida M *et al* 2007 *Nucl. Fusion* **47** 856
[11] Tala T *et al* 2009 *Phys. Rev. Lett.* **102** 075001
[12] Kaye S M *et al* 2009 *Nucl. Fusion* **49** 045010
[13] Solomon W M *et al* 2009 *Nucl. Fusion* **49** 085005
[14] Zastrow K-D *et al* 1998 *Nucl. Fusion* **38** 257
[15] de Vries P C *et al* 2008 *Nucl. Fusion* **48** 035007
[16] Rice J E *et al* 2004 *Nucl. Fusion* **44** 379
[17] Rice J E *et al* 2007 *Nucl. Fusion* **47** 1618
[18] Solomon W M *et al* 2007 *Plasma Phys. Control. Fusion* **49** B313
[19] Oyama N *et al* 2008 *J. Phys. Conf. Ser.* **123** 012015
[20] Saibene G *et al* 2008 *Proc. 22nd Int. Conf. on Fusion Energy 2008 (Geneva, Switzerland, 2008)* (Vienna: IAEA) CD-ROM file EX/2-1 http://www-naweb.iaea.org/napc/physics/ FEC/FEC2008/papers/ex_2-1.pdf
[21] Yoshida M *et al* 2006 *Plasma Phys. Control. Fusion* **48** 1673
[22] Salmi A *et al* 2008 *Contrib. Plasma Phys.* **48** 77
[23] Nave M F F *et al* 2009 *Proc. 36th EPS Conf. on Plasma Physics (Sofia, Bulgaria)* vol 33E (ECA) P-2.168 http://epsppd.epfl.ch/Sofia/ pdf/P2_168.pdf
[24] Cole A J, Hegna C C and Callen J D 2008 *Phys. Plasmas* **15** 056102
[25] Diamond P H *et al* 2009 *Nucl. Fusion* **49** 045002
[26] Camenen Y *et al* 2009 *Phys. Rev. Lett.* **102** 125001
[27] Tala T *et al* 2007 *Plasma Phys. Control. Fusion* **49** B291